INTERNATIONAL JOURNAL FOR NUMERICAL METHODS IN FLUIDS, VOL. 5, 347–356 (1985)

A METHOD FOR PREDICTING UNSTEADY POTENTIAL FLOW ABOUT AN AEROFOIL

M. VEZZA AND R. A. McD. GALBRAITH

Department of Aeronautics and Fluid Mechanics, Glasgow University, Glasgow, Scotland

SUMMARY

A new model is presented for the calculation of the incompressible, inviscid flow around an arbitrary aerofoil undergoing unsteady motion. The technique was developed from the steady flow algorithm of Leishman and Galbraith[1] in which use was made of a linear distribution of panel vorticity. The procedure is in the same class as that of Basu and Hancock[2] but, because of the particular approach to the manner of specifying the shed vorticity, only a set of linear simultaneous equations needs be solved, unlike the method of Reference 2, complicated by the necessary solution of a quadratic.

A brief history of unsteady flow modelling is given in the introduction, followed by the mathematical details of the current method. Results are presented and discussed for a number of cases which clearly illustrate relevant characteristics of unsteady flow.

KEY WORDS Aerofoils Unsteady Potential Discrete Vortex Two-dimensional

INTRODUCTION

For some time, aerodynamicists have recognized that unsteady flow over lifting bodies can produce beneficial effects, e.g. the phenomenon of stall delay,[3] and this has encouraged both theoretical and experimental studies, with the aim of improving the performance of turbomachinery, helicopter rotors and wind turbines, etc.

Among the first unsteady potential theories were those developed by von Karman and Sears[4] and Theodorsen[5] who considered a thin flat plate executing small amplitude, simple harmonic motions. Solutions for these linear problems can be expressed in terms of combinations of standard Bessel functions with argument k (the reduced frequency of oscillation). Flat plate solutions for transient motions were developed by Wagner[6] and Küssner,[7] but again second order effects were omitted. Thickness effects have been considered for small amplitude oscillations by Küssner,[8] van de Vooren and van de Vel[9] and Hewson-Brown.[10] These, however, were based on conformal mapping techniques and were limited to particular aerofil geometries.

In recent years, the availability of greater computational power has encouraged the development of numerical methods for the assessment of unsteady flows. The most fundamental was developed by Giesing[11] and is based on the steady model of Hess and Smith.[12] This general, non-linear, potential flow method was applied step by step in time along the aerofoil flight path, starting from an initial position and orientation, and the non-linear rolled up wake pattern evolved naturally in the solution. Basu and Hancock[2] adapted and simplified Giesing's method and applied it to a number of different cases which illustrate the characteristics of unsteady flow. The Kutta condition used was the specification of zero loading across the trailing edge rather than smooth outflow, as included in Giesing's[11] model. Basu and Hancock argued, however,

0271–2091/85/040347–10$01.00

Received 16 April 1984
Revised 10 July 1984

that ideally both conditions could be satisfied if, as postulated by Maskell,[13] the shed vorticity left the trailing-edge parallel to one or other of the surfaces, depending on the sign.

The model presented in this paper is based on the steady flow algorithm of Leishman and Galbraith[1] and makes use of a linear distribution of panel vorticity which is piecewise continuous at the panel corners. In the steady case, the system of linear simultaneous equations may be reduced to

$$\mathbf{U}_\infty \cdot \hat{\mathbf{n}}_i + \sum_{j=1}^{N+1} A_{ij}\gamma_j = 0, \qquad i = 1, 2, 3, \ldots, N$$

where the summation term is the induced normal velocity due to the vortex sheet. The condition of zero loading across the trailing edge gives

$$\gamma_1 + \gamma_{N+1} = 0$$

The potential formulation was seen as a first step towards the incorporation of viscous effects so that a more accurate model of trailing-edge dynamic stall can be obtained.

THEORETICAL DESCRIPTION OF THE MODEL

The unsteady flow problem is solved at successive intervals of time starting with the steady solution at $t = 0$. At time t_m the panel and shed vortices are as illustrated in Figure 1. The aerofoil is represented by N panels, from upper to lower trailing-edge, across which there is a linear distribution of vorticity and the total circulation around the contour is Γ_m, where $\Gamma_m = \int_C \gamma_s \, ds$. The vorticity shed at earlier times is represented by discrete vortices which convect down stream according to the induced velocity pertaining to each.

The shed vorticity at time t_m manifests itself as an extra panel, attached to the trailing-edge of length Δ_m, inclination θ_m and a constant strength which is specified by making use of Helmholtz's theorem[14] of continuity of vorticity. This is related to the change in aerofoil circulation, thus

$$\Delta_m(\gamma_1 + \gamma_{N+1}) = \Gamma_{m-1} - \Gamma_m$$

At time t_m therefore there are $N + 3$ unknowns, i.e. $N + 1$ values of vorticity, θ_m and Δ_m, but only N equations of zero normal flow, and one equation specifying the shed vorticity.

To obtain a solution, θ_m and Δ_m have to be obtained by iteration from an initial guess.

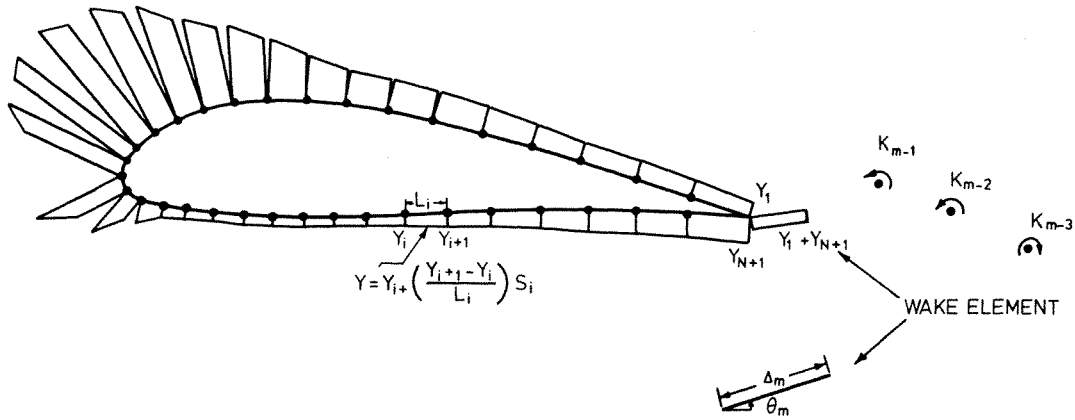

Figure 1. Unsteady model at time t_m

The N conditions of zero normal flow, applied at the panel mid-points (control points), can be reduced to

$$\mathbf{U}_\infty \cdot \hat{\mathbf{n}}_i + \sum_{j=1}^{N+1} A_{ij}\gamma_j + \sum_{p=1}^{m-1} B_{ip}K_p + (\gamma_1 + \gamma_{N+1})A_{wi} - \mathbf{V}_r \cdot \hat{\mathbf{n}}_i = 0, \quad i = 1, 2, \ldots, N \tag{1}$$

where the relevant components are due to the free stream, the bound vortex sheet, the wake vortices, the extra trailing-edge panel and the moving boundary. The condition of zero loading across the trailing-edge is obtained from the unsteady Bernoulli equation:

$$\frac{p_1 - p_{N+1}}{\rho} = 0 = \tfrac{1}{2}\gamma_{N+1}^2 - \tfrac{1}{2}\gamma_1^2 + \frac{\partial(\Phi_{N+1} - \Phi_1)}{\partial t}$$

i.e.

$$\frac{\partial(\Phi_{N+1} - \Phi_1)}{\partial t} = \tfrac{1}{2}(\gamma_1^2 - \gamma_{N+1}^2) = \frac{\partial \Gamma_m}{\partial t} \text{ as } \Gamma_m = \Phi_{N+1} - \Phi_1. \tag{2}$$

Once Δ_m and θ_m have been assumed, a solution is obtained by solving the $N+1$ linear simultaneous equations for the vorticity values $\gamma_1 \rightarrow \gamma_{N+1}$ using the largest pivotal divisor elimination technique. The induced velocity at the control point of the extra trailing-edge panel may then be calculated and a more accurate value of θ_m obtained by ensuring that the shed vorticity leaves the trailing-edge along the local streamline, i.e.

$$\theta_m = \tan^{-1}\left(\frac{V_{w_m}}{U_{w_m}}\right)$$

A new value of Δ_m is obtained by ensuring that the condition of zero loading is satisfied

$$\tfrac{1}{2}(\gamma_{N+1}^2 - \gamma_1^2)(t_m - t_{m-1}) = (\gamma_1 + \gamma_{N+1})\Delta_m$$

i.e.

$$\Delta_m = \tfrac{1}{2}(\gamma_{N+1} - \gamma_1)(t_m - t_{m-1})$$

The above procedure is repeated until θ_m and Δ_m converge.

The unsteady pressure coefficient follows directly from the Bernoulli equation for a moving co-ordinate system;

$$C_p = 1 + \frac{V_r^2}{U_\infty^2} - \frac{\gamma^2}{U_\infty^2} - \frac{2}{U_\infty^2}\frac{\partial \Phi}{\partial t}$$

The potential function is approximated by integrating the velocity field, as viewed in the moving frame, from upstream of the aerofoil to the leading edge and then around the surface.

One the calculation at time t_m has converged, the procedure is then set up for time t_{m+1}. The wake vortices are convected to their new positions, determined by the induced velocity at their centres and the extra trailing-edge panel is located as a point vortex in the wake thus:

$$x_v = x_{cw} + U_{wm}(t_{m+1} - t_m)$$
$$y_v = y_{cw} + V_{wm}(t_{m+1} - t_m)$$

Normally the aerofoil would also be rotated to its new position at time t_{m+1}; however, for the present model, the stream is rotated along with any wake vortices and upstream reference point, so that the influence co-efficients due to the bound vortex sheet need only be calculated once at the start and thereafter remain unchanged.

RESULTS AND DISCUSSION

The above method has been applied to a number of unsteady flows, e.g. (i) a step change in incidence, (ii) sinusoidal oscillations and (iii) ramp motions.

(i) *Step change in incidence (0–5°)*

The above method was employed to consider the NACA 0012 aerofoil undergoing a sudden change in incidence from 0° to 5°. This motion represents the particular case of the time-dependent built-up in lift as well as the phenomenon of the starting vortex.

The solution was obtained with short time intervals of 0·01 for $0 < \Delta t U_\infty/c < 0{\cdot}3$, intervals of 0·05 for $0{\cdot}3 < \Delta t U_\infty/c < 0{\cdot}5$, 0·1 for $0{\cdot}5 < \Delta t U_\infty/c < 2{\cdot}0$ and finally intervals of 0·2 for $2{\cdot}0 < \Delta t U_\infty/c < 20{\cdot}0$. Inherent in this problem is an initial transient value of lift due to the instantaneous change in aerofoil angle of attack; but no account has been taken of this, and the solution originates when the lift returns to a low value. Figure 2(a) illustrates the results obtained for the built-up in pressure on the NACA 0012 aerofoil. The evident built-up to the steady state condition is further highlighted in Figure 2(b), which illustrates the behaviour of the time dependent lift, i.e. very rapid increase over a short period followed by a more gradual increase towards the steady-state value. Figure 2(c) shows how the starting vortex comes off the trailing-edge, convects downstream and rolls up in the characteristic way. Although this is not a true representation of that which actually happens, i.e. the vortex originating at the trailing edge, its subsequent development is good.

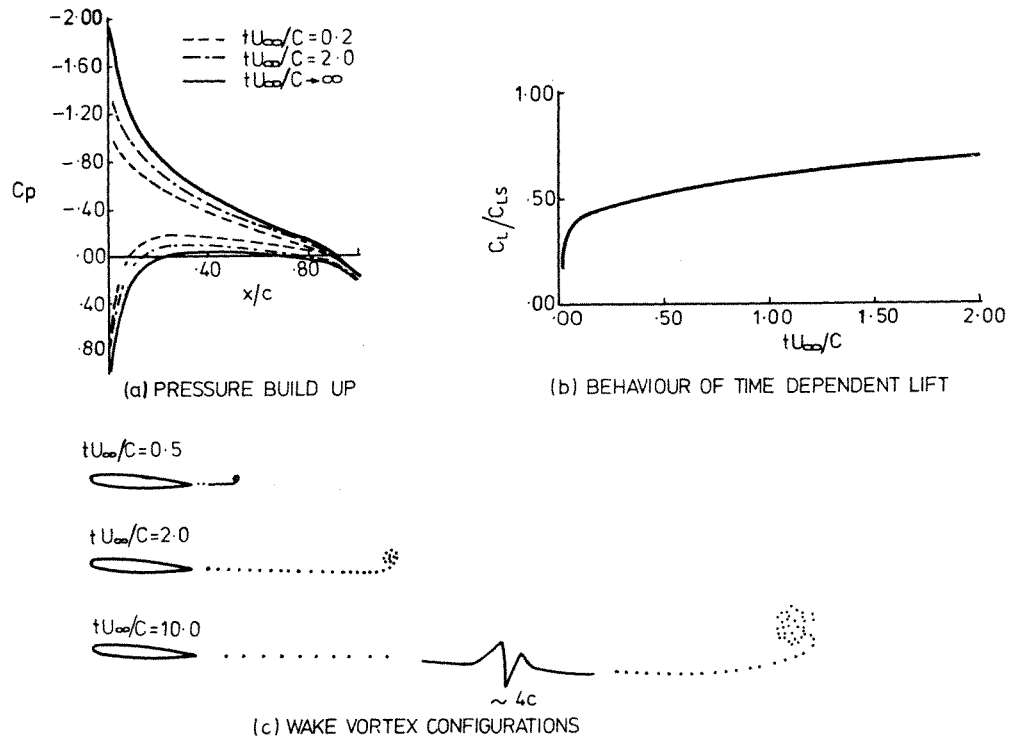

Figure 2. Results obtained following a step change in incidence from 0–5° using the NACA 0012 aerofoil

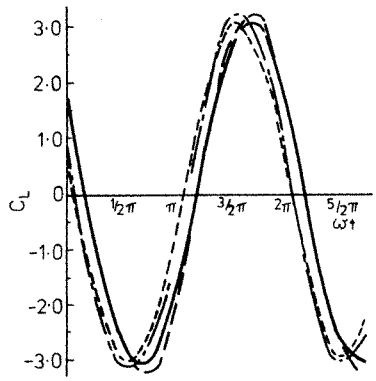

(a) BEHAVIOUR OF TIME DEPENDENT LIFT; $\theta = 0{\cdot}573° \sin 20t$ ABOUT ℓ.e.

———— PRESENT METHOD
——— BASU AND HANCOCK[2]
—·— BASU AND HANCOCK[15]
- - - - - LINEARISED THEORY

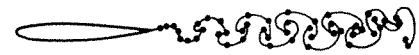

$\theta = 0{\cdot}573° \sin 20t$ ABOUT LEADING EDGE OF NACA 0012 AEROFOIL.

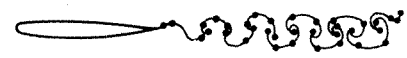

$\theta = 0{\cdot}573° \sin 20t$ ABOUT LEADING EDGE OF 8·4% SYMMETRICAL VON MISES AEROFOIL[2]

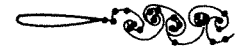

$W_y = 0{\cdot}3105 \cos 17t$ FOR NACA 0015 AEROFOIL.

(b) WAKE VORTEX CONFIGURATIONS.

Figure 3. Results obtained from high frequency calculations

(ii) *Sinusoidal oscillations*

Again using the NACA 0012 aerofoil a solution was obtained for sinusoidal oscillations about the leading edge at a reduced frequency of $\omega c/2U_\infty = 10$, a mean angle of 0° and amplitude 0·573° using a time step $\Delta t U_\infty/c = 0{\cdot}03927$ from zero to a time $tU_\infty/c = 1{\cdot}88496$.

Figure 3(a) illustrates the behaviour of the lift after the initial transients had faded and the response was repeatable. The very large values of this parameter were due to the high oscillation frequency, not unlike that encountered during aerofoil 'flutter'. However, not only is there a magnification of the load over the steady case, but a large lag exists of more than 180° as is shown by the initially decreasing lift values. This may be attributed to the large rates of change of the potential as well as the above mentioned motion effect. The lift variations attributable to the Basu and Hancock model, to an earlier linearized model[15] by the same authors, and to the standard linearized solution are also illustrated.

At high frequencies a very strong vortex sheet is shed from the trailing edge, as can be seen from the highly deformed wake pattern shown in Figure 3b. Also shown are the resulting wakes of similar tests carried out by both Basu and Hancock[2] and Giesing,[11] which further illustrate the highly non-linear nature of the problem.

Other sinusoidal tests of particular interest are low frequency, large mean angle and amplitude oscillations about the 1/4 chord which are typical of helicopter rotor motions.

Figure 4(a) illustrates some recent results obtained from experiment[16] and theory for a test carried out on a NACA 23012 aerofoil at a reduced frequency of 0·2, an amplitude of 6° and a mean angle of 10°. The Reynolds number and free-stream Mach number of the test were $1{\cdot}027 \times 10^6$ and 0·076, respectively, and the data were averaged over 10 cycles. The theoretical computation was carried out using a time step $\Delta t U_\infty/c = 0{\cdot}3141$ from zero to a time $tU_\infty/c = 31{\cdot}41$ which corresponds to two complete cycles, the second of which is shown. Although there appears to be poor agreement between the two results, this may be attributed to the relatively low Reynolds number at which the experiment was carried out. As may be seen from Figure 4(b),[17] this particular aerofoil exhibits a marked variation of c_L with Reynold's number. Taking account of this

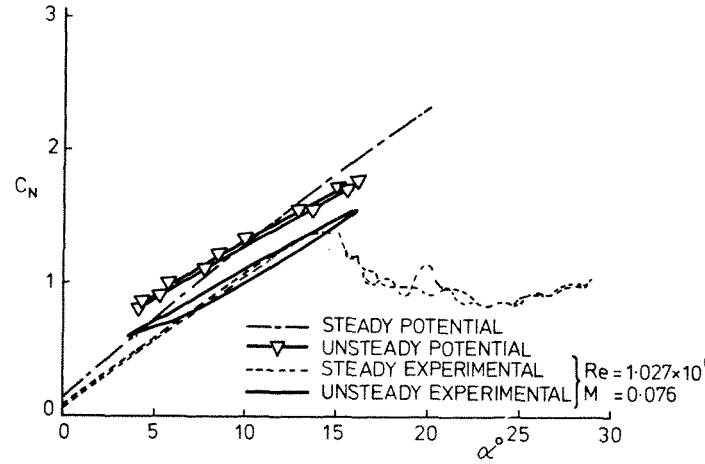

(a) NORMAL LIFT CHARACTERISTICS FOR OSCILLATION ABOUT THE ¼c OF THE NACA 23012 AEROFOIL; $k = 0{\cdot}2$, $\alpha = 10° + 6° \sin \omega t$

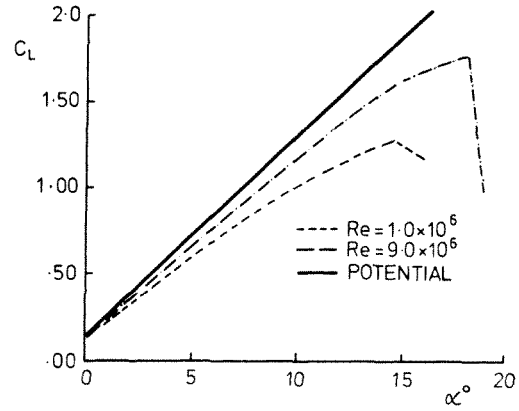

(b) VARIATION OF C_L vs α WITH REYNOLDS NUMBER FOR THE NACA 23012 AEROFOIL.

Figure 4. Comparison of results obtained from a low frequency sub-stall test on the NACA 23012 aerofoil

variation, the results presented in Figure 4(a) are very encouraging in that the experimental lift loop has been reproduced theoretically as has the relative orientation to the static line, both phenomenon being due to the motion of the aerofoil and the time rate of change of the potential. The curvature of the static C_N vs α curve is due to relatively large negative profile drags at the higher angles of attack.

The above comparison illustrates how the unsteady potential model reproduces the characteristic lift behaviour when viscous effects are not of first order in magnitude; however, when the aerofoil motion induces the classic effects of dynamic stall then few recognizable features can be reproduced. Figure 5 illustrates this with results obtained from a test carried out on the same aerofoil at a reduced frequency of 0·2, an amplitude of 10° and a mean angle of 13°. The experimental Reynolds number and free-stream Mach number were $1{\cdot}036 \times 10^6$ and 0·077, respectively, and the same time variation and limit were used in the theoretical model. It can be seen that the omission of unsteady separation from the model limits its applicability, although the lift variation during the upstroke has been reproduced fairly well.

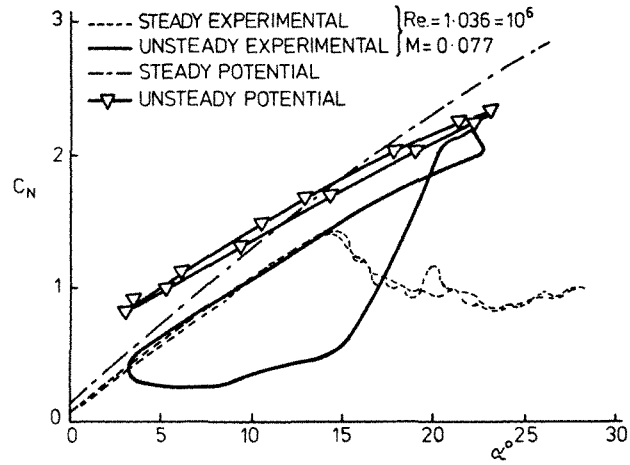

Figure 5. Comparison of normal lift on the NACA 23012 aerofoil when operating in the stall regime: $\kappa = 0{\cdot}2$, $\alpha = 13° + 10° \sin \omega t$

(iii) *Ramp motions*

The ramp tests consisted of rotating an aerofoil, about the 1/4 chord, at a constant angular velocity. The experimental tests incorporated angular acceleration up to the constant rate, whereas for the present calculation an 'ideal' ramp was used. Figure 6 compares the experimental[18] and theoretical results obtained from tests carried out on the NACA 0012 aerofil at reduced ramp rates $\dot{\alpha}c/2U_\infty = 0{\cdot}0016$ and $0{\cdot}0065$. The experimental Reynolds number and free-stream Mach number were $2{\cdot}6 \times 10^6$ and $0{\cdot}3$ respectively. This Mach number represents approximately the upper limit of applicability of incompressible theory without significant error being incurred. The theoretical tests were carried out using time steps $\Delta t U_\infty/c = 0{\cdot}4363$ for the test at $\dot{\alpha}c/2U_\infty = 0{\cdot}0016$ and $\Delta t U_\infty/c = 0{\cdot}3222$ for the test at $\dot{\alpha}c/2U_\infty = 0{\cdot}0065$.

For ease of comparison the experimental curves represent smoothed values of C_N and as can be seen, the correlation with the predicted values is very good. Analogous to the sinusoidal cases mentioned earlier, the effect of increasing the reduced ramp rate is to modify the slopes of the lift curves, representing an increase in the lag of response.

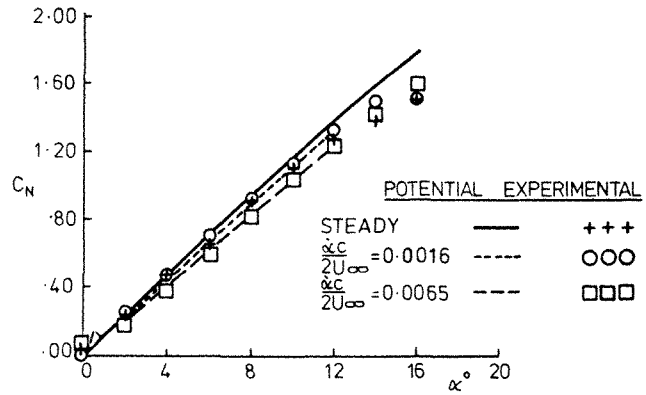

Figure 6. Resulting normal lift variations with incidence when ramp motions are applied to the NACA 0012 aerofoil for experiments: $Re = 2{\cdot}6 \times 10^6$, $M = 0{\cdot}3$

The initial small peak in the predicted lift for the test at $\dot{\alpha}c/2U_\infty = 0{\cdot}0065$ is due to the abrupt start up mentioned earlier. Also shown in Figure 6 are the predicted and experimental ($Re = 3 \times 10^6$) static curves. The agreement in this case is much better than that obtained with the 23012 and may be attributed to the observed insensitivity of this profile to the Reynolds number over the given range.[17]

COMPUTATIONAL DETAILS

The decision on the number of panels that should be used to represent an aerofoil was based on compromise between accuracy on the one hand and time to perform the task required on the other. In general the size of panel to be used is inversely proportional to the surface curvature which means, for the aerofoils presented in this paper, concentration of panels around the leading-edge. This was accomplished by using the following analytic expression for the corner points:

$$x_i = 1 - \cos\theta_i, \quad \theta_i = \frac{\pi}{N}(i-1), \quad i = 1, \ldots, N/2+1, \quad N \text{ even}$$

The y co-ordinates were then calculated from the available analytic functions for the respective NACA profiles. Tests using the potential flow program[1] with values of N up to 70 show that below $N = 30$, the results obtained deviate significantly from those obtained using between 30–70 panels.

Therefore, bearing in mind that the time taken to solve the matrix of co-efficients is proportional to N^3, a 30-panel representation of the aerofoils was used for the tests presented herein. The reference potential point is initially located three chord lengths upstream from the leading-edge and the change in potential calculated across each of 30 equal length panels up to the aerofoil. The choice of what time step value $\Delta t U_\infty/c$ to employ was obtained by balancing the computational time incurred with the accuracy of the results. Larger time steps were used in the lower frequency tests where the induced velocities were not as great.

Only four wake iterations were carried out per time step since thereafter both the length and orientation of the extra trailing-edge panel showed little change. Note that the computational details of the coding of the equivalent Basu and Hancock model are given in Reference 19.

CONCLUSIONS

A successful method for calculating the unsteady, incompressible potential flow around an arbitrary aerofoil has been developed. The method uses a linear distribution of panel vorticity on the aerofoil surface and a new way of shedding the necessary vorticity into the free stream in the form of discrete vortices. This particular feature yields a simpler algorithm than that of Reference 2.

From the preceding discusion it may be concluded that the method predicts fully attached potential flow about an aerofoil, but it is inappropriate where significant viscous effects, e.g. marked Reynolds number dependence and separation, are present.

ACKNOWLEDGEMENTS

The authors wish to thank the U.K. Science & Engineering Research Council (S.E.R.C.) for the use of the GEC4070 computer and the Glasgow University Engineering computing staff for their assistance. The work was funded under S.E.R.C Grant No. 82801965.

SYMBOL GLOSSARY

A	influence coefficient
α	angle of attack
$\dot{\alpha}$	angular velocity
B_{ip}	wake vortex coefficient
c	chord length
C_N	normal lift coefficient
C_M	moment coefficient
C_L	lift coefficient
C_p	pressure coefficient
γ	vorticity strength
Γ	circulation
Δ, θ	length and orientation of extra trailing edge panel
Φ	velocity potential
k	reduced frequency
K	free vortex strength
L	panel length
M	Mach number
N	number of panels representing aerofoil
$\hat{\mathbf{n}}$	unit normal vector
p	pressure
ρ	density
Re	Reynolds number
$t, \Delta t$	time
$\mathbf{U}_\infty$	free stream velocity
U, V	velocity components
$\mathbf{V}_r$	velocity of point fixed to aerofoil
ω	frequency of oscillation
x, y	cartesian co-ordinates

Subscripts

c	control point
i, j	index of aerofoil surface elements
LE	leading edge
m	time step counter
s	steady flow
v	wake vortex
w	extra trailing edge panel
$\frac{1}{4}$	quarter chord

REFERENCES

1. J. G. Leishman and R. A. McD. Galbraith, 'An algorithm for the calculation of the potential flow about an arbitrary two-dimensional aerofoil', *G. U. Report No. 8102*, May 1981.
2. B. C. Basu and G. J. Hancock, 'The unsteady motion of a two-dimensional aerofoil in incompressible, inviscid flow', *J. Fluid Mech.*, **87**, (Part 1), 159–178 (1978).
3. F. O. Carta, 'Effect of unsteady pressure gradient reduction on dynamic stall delay', *J. Aircraft*, **8**, (10), (1971).
4. T. von Karman and W. R. Sears, 'Airfoil theory for non-uniform motion', *Journal of Aeronautical Sciences*, **5**, 379–390 (1938).

5. T. Theodorsen, 'General theory of aerodynamic instability and the mechanism of flutter', *NACA Report 496*, 1935.
6. H. Wagner, 'Dynamischer auftrieb von tragflügelin', *Zeitshrift fuer Angewandte Mathematik und Mechanik*, **5,** 17 (1925).
7. H. G. Küssner, 'Das zweidimensionale problem der beliebig bewegten tragfläche unter berücksichtigung von partial bewegungen der flüssigkeit', *Luftfahrtfarschung*, **17,** 355 (1940).
8. H. G. Küssner, 'Nonstationary theory of airfoils of finite thickness in incompressible flow', *AGARD Manual on Aeroelasticity*, Part II, Neuilly-sur-Seine, France, 1960, Chap. 8.
9. A. I. van de Vooren and H. van de Vel, 'Unsteady profile theory in incompressible flow', *Arch. Mech. Stososanej*, **16,** 709–735 (1964).
10. R. C. Hewson-Brown, 'The oscillation of a thick aerofoil in an incompressible flow', *Mechanics and Applied Mathematics*, **16,** (1963).
11. J. P. Giesing, 'Nonlinear two-dimensional unsteady potential flow with lift', *J. Aircraft*, **5,** (2), (1968).
12. J. L. Hess and A. M. O. Smith, 'Calculations of potential flow about arbitrary bodies', *Prog. Aero. Sci.*, **8,** (1), (1967).
13. E. C. Maskell, 'On the Kutta–Joukowski condition in two-dimensional unsteady flow', Unpublished Note, Royal Aircraft Establishment, Farnborough, 1972.
14. L. M. Milne Thompson, *Theoretical Aerodynamics*, Dover Publications Inc., New York, 4th Edition, pp. 168–169.
15. B. C. Basu and G. J. Hancock, 'Two-dimensional aerofoils and control surfaces in simple harmonic motion in incompressible inviscid flow', Aero Res. Council, *CP 1392*, 1978.
16. R. A. McD. Galbraith and J. G. Leishman, Private Communication, 1983.
17. L. K. Loftin, Jr. and H. A. Smith, 'Aerodynamic characteristics of 15 NACA airofoil sections at seven Reynolds numbers from $0{\cdot}7 \times 10^6$ to $9{\cdot}0 \times 10^6$', *NACA TN 1945*, 1949.
18. A.R.A. Private Communication, 1983.
19. M. Vezza and R. A. McD. Galbraith, 'An algorithm for the prediction of unsteady potential flow about an arbitrary aerofoil', *G.U. Aero. Report No. 8306*, October 1983.